

Global Biogeochemical Cycles

Supporting Information for

The modeled seasonal cycles of surface N₂O fluxes and atmospheric N₂O

Qing Sun^{1,2}, Fortunat Joos^{1,2}, Sebastian Lienert^{1,2}, Sarah Berthet³, Dustin Carroll⁴, Cheng Gong⁵, Akihiko Ito^{6,7}, Atul K. Jain⁸, Sian Kou-Giesbrecht^{9,10}, Angela Landolfi¹¹, Manfredi Manizza¹², Naiqing Pan^{13,14}, Michael Prather¹⁵, Pierre Regnier¹⁶, Laure Resplandy¹⁷, Roland Séférian³, Hao Shi¹⁸, Parvatha Suntharalingam¹⁹, Rona L. Thompson²⁰, Hanqin Tian^{13,14}, Nicolas Vuichard²¹, Sönke Zaehle⁵, Qing Zhu²²

¹ Climate and Environmental Physics, Physics Institute, University of Bern, Bern, Switzerland

² Oeschger Centre for Climate Change Research, University of Bern, Bern, Switzerland

³ CNRM, Université de Toulouse, Météo France, CNRS, Toulouse, France

⁴ Moss Landing Marine Laboratories, San José State University, Moss Landing, California, USA

⁵ Biogeochemical Signals Department, Max Planck Institute for Biogeochemistry, Jena, Germany

⁶ Graduate School of Life and Agricultural Sciences, University of Tokyo, Tokyo, Japan

⁷ Earth System Division, National Institute for Environmental Studies, Tsukuba, Japan

⁸ Department of Atmospheric Sciences, University of Illinois, Urbana-Champaign, Urbana, IL61801, USA

⁹ Department of Earth and Environmental Sciences, Dalhousie University, Halifax, NS, Canada

¹⁰ Canadian Centre for Climate Modelling and Analysis, Environment and Climate Change Canada, Victoria, BC, Canada

¹¹ National Research Council, Institute of Marine Sciences (ISMAR-CNR- ISMAR), Via Fosso del Cavaliere 100, Rome, Italy

¹² Geosciences Research Division, Scripps Institution of Oceanography, University of California- San Diego, La Jolla, CA

¹³ Schiller Institute for Integrated Science and Society, Department of Earth and Environmental Sciences, Boston College, Chestnut Hill, MA 02467, USA

¹⁴ International Center for Climate and Global Change Research, College of Forestry, Wildlife and Environment, Auburn University, Auburn 36830, USA

¹⁵ Department of Earth System Science, University of California Irvine, Irvine, CA, USA

¹⁶ Department Geoscience, Environment & Society - BGEO SYS, Université Libre de Bruxelles, 1050-Brussels, Belgium

¹⁷ Princeton University, Geosciences Department, High Meadows Environmental Institute, Princeton, NJ, USA

¹⁸ State Key Laboratory of Urban and Regional Ecology, Research Center for Eco-Environmental Sciences, Chinese Academy of Sciences, Beijing 100085, China

¹⁹ Centre for Ocean and Atmospheric Sciences, School of Environmental Sciences, University of East Anglia, NR4 7TJ, United Kingdom

²⁰ NILU, 2007 Kjeller, Norway

²¹ Laboratoire des Sciences du Climat et de l'Environnement, LSCE-IPSL (CEA-CNRS-UVSQ), Université Paris-Saclay 91191 Gif-sur-Yvette, France

²² Climate and Ecosystem Sciences Division, Lawrence Berkeley National Lab, 1 Cyclotron Road, Berkeley, CA 94720, USA

Contents of this file

Table S1. Modeled seasonal amplitude of tropospheric N₂O mixing ratio from seasonality and spatial pattern of N₂O fluxes

Figure S1. Modeled aN₂O seasonality at different NOAA/CCGG flask stations from land and ocean surface fluxes and anthropogenic activities by EDGAR

Figure S2. Model spread for NMIP-2 land models and ocean models in N₂O emission density

Figure S3. Modeled aN₂O seasonality at different NOAA/CCGG flask stations from spatial and seasonality of N₂O fluxes

Table S1. Modeled seasonal min-to-max amplitude of tropospheric N₂O mixing ratio (ppb; multi-model median [25th percentile, 75th percentile] derived from long-term model average of modeled aN₂O seasonal cycle) from spatial pattern, using 12-month running mean, as well as seasonality, using detrended fluxes, of land and ocean N₂O fluxes at NOAA/CCGG stations (ALT: Alert, BRW: Barrow, AZR: Terceira Island, RPB: Ragged Point, CHR: Christmas Island, ASC: Ascension Island, SMO: Samoa, CGO: Cape Grim). The seasonal amplitude attributed to total of land and ocean emissions as well as separated are given. Pre-industrial N₂O fluxes from the ocean are only available for Bern3D.

Site	Present day (2001-2020)			Pre-industrial (1861-1880)		
	Land + ocean	Land	Ocean	Land + ocean	Land	Ocean
Seasonal amplitude from spatial pattern of N ₂ O fluxes						
ALT	0.17 [0.13, 0.23]	0.18 [0.13, 0.22]	0.04 [0.03, 0.04]	0.11 [0.10, 0.15]	0.11 [0.09, 0.15]	0.02
BRW	0.17 [0.14, 0.23]	0.18 [0.13, 0.23]	0.07 [0.05, 0.09]	0.12 [0.10, 0.16]	0.13 [0.08, 0.16]	0.05
AZR	0.17 [0.13, 0.22]	0.17 [0.12, 0.21]	0.05 [0.04, 0.07]	0.12 [0.10, 0.17]	0.11 [0.10, 0.15]	0.03
RPB	0.21 [0.16, 0.28]	0.24 [0.16, 0.28]	0.06 [0.04, 0.09]	0.25 [0.22, 0.29]	0.18 [0.14, 0.22]	0.11
CHR	0.41 [0.31, 0.47]	0.45 [0.33, 0.49]	0.11 [0.09, 0.14]	0.28 [0.23, 0.32]	0.20 [0.16, 0.23]	0.15
ASC	0.35 [0.31, 0.39]	0.34 [0.30, 0.37]	0.07 [0.04, 0.10]	0.36 [0.33, 0.38]	0.27 [0.25, 0.31]	0.09
SMO	0.28 [0.24, 0.35]	0.25 [0.24, 0.32]	0.05 [0.04, 0.06]	0.19 [0.14, 0.24]	0.18 [0.12, 0.21]	0.04
CGO	0.14 [0.11, 0.20]	0.19 [0.16, 0.23]	0.06 [0.06, 0.08]	0.08 [0.07, 0.14]	0.13 [0.11, 0.16]	0.07
Seasonal amplitude from seasonality of N ₂ O fluxes						
ALT	0.66 [0.59, 0.80]	0.69 [0.64, 0.86]	0.16 [0.15, 0.17]	0.43 [0.39, 0.46]	0.45 [0.40, 0.51]	0.13
BRW	0.71 [0.60, 0.82]	0.73 [0.68, 0.89]	0.17 [0.16, 0.18]	0.42 [0.40, 0.49]	0.46 [0.42, 0.53]	0.14
AZR	0.58 [0.51, 0.66]	0.65 [0.60, 0.74]	0.21 [0.14, 0.28]	0.35 [0.32, 0.38]	0.43 [0.36, 0.47]	0.16
RPB	0.46 [0.37, 0.66]	0.51 [0.41, 0.69]	0.14 [0.11, 0.18]	0.32 [0.25, 0.40]	0.34 [0.29, 0.39]	0.09
CHR	0.31 [0.25, 0.35]	0.31 [0.21, 0.33]	0.11 [0.10, 0.13]	0.13 [0.11, 0.23]	0.19 [0.13, 0.24]	0.11
ASC	0.28 [0.23, 0.38]	0.25 [0.22, 0.31]	0.20 [0.17, 0.20]	0.21 [0.17, 0.26]	0.22 [0.18, 0.31]	0.22
SMO	0.23 [0.20, 0.32]	0.18 [0.13, 0.26]	0.14 [0.14, 0.16]	0.17 [0.14, 0.23]	0.12 [0.10, 0.24]	0.16
CGO	0.28 [0.23, 0.34]	0.21 [0.15, 0.26]	0.22 [0.21, 0.24]	0.22 [0.19, 0.26]	0.12 [0.11, 0.24]	0.21

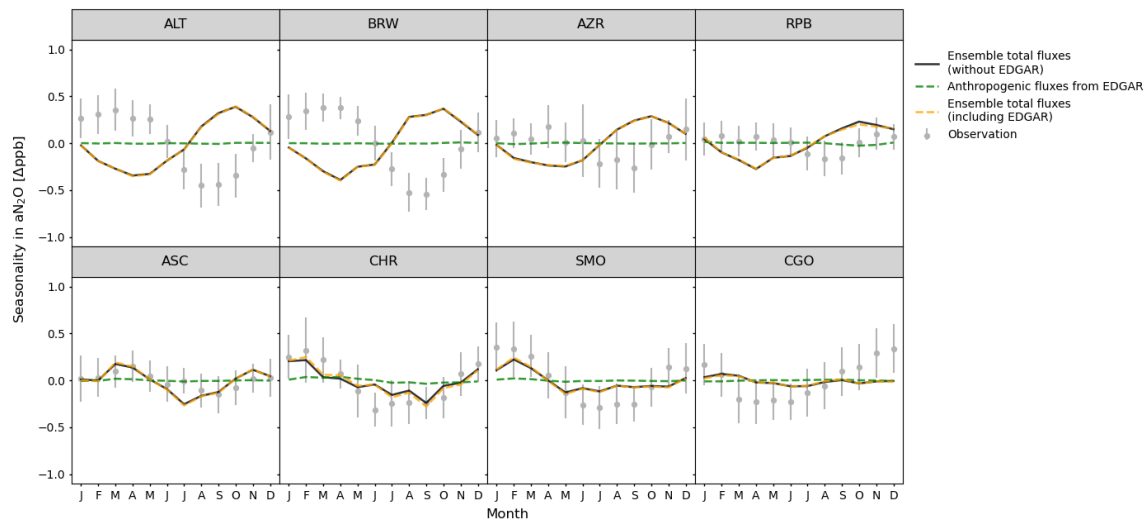


Figure S1. Long-term average seasonality of observed aN₂O (solid grey circles) and modeled aN₂O (lines) for present-day (2001-2020) at different NOAA/CCGG flask stations (ALT: Alert, BRW: Barrow, AZR: Terceira Island, RPB: Ragged Point, ASC: Ascension Island, CHR: Christmas Island, SMO: Samoa, CGO: Cape Grim). Modeled aN₂O seasonality is attributed to the N₂O emissions from ensemble median of land and ocean surface fluxes without EDGAR data (solid black lines), other anthropogenic activities by EDGARv8.0 [EDGAR, 2023] (https://edgar.jrc.ec.europa.eu/dataset_ghg80) (dashed green lines), ensemble median of land and ocean surface fluxes with EDGAR emissions (dashed orange lines). Vertical lines on grey circles indicate observed temporal variability weighted with measurement uncertainty. The modeled aN₂O seasonal amplitude from other anthropogenic activities from the EDGARv8.0 data only ranges from 0.01 to 0.07 ppb and is negligible in comparison with amplitudes from land, ocean, and stratospheric fluxes and their uncertainties.

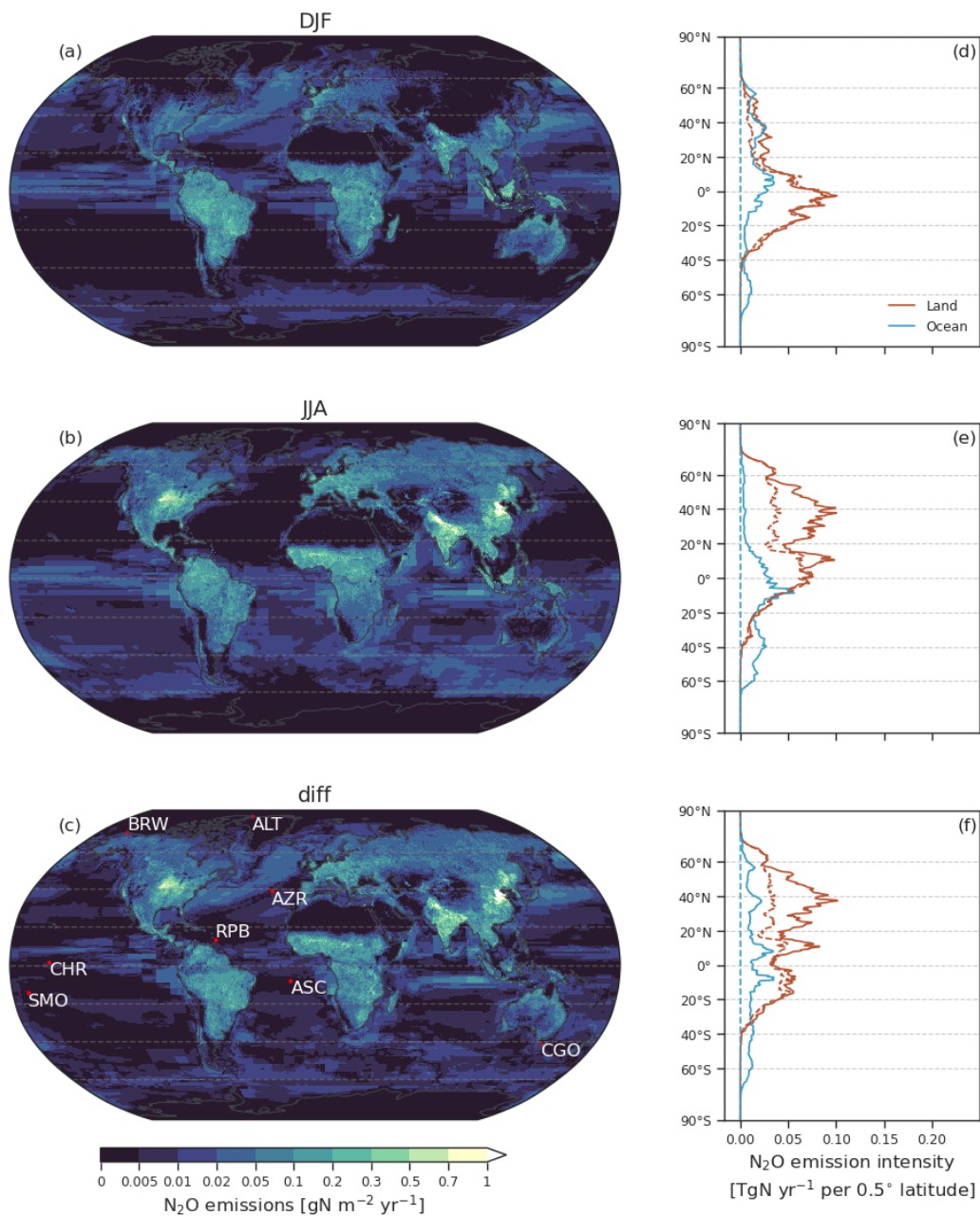


Figure S2. Model spread for NMIP-2 land models and ocean models in N₂O emission density ($\text{gN m}^{-2} \text{yr}^{-1}$) during present day (2001 to 2020) for DJF (a, December, January, and February), JJA (b, June, July, and August), and the absolute differences between these two seasons (c) as well as the spread (TgN yr^{-1}) along the latitudinal gradient resolved by 0.5° for both the land (red lines) and the ocean (blue lines) during PD (solid lines) and pre-industrial period (PI; 1861-1880, dashed lines) (d, e, f). The selected NOAA/CCGG stations are marked by red points in (c) (ALT: Alert, BRW: Barrow, CGO: Cape Grim, AZR: Terceira Island, RPB: Ragged Point, CHR: Christmas Island, SMO: Samoa, ASC: Ascension Island). The interquartile ranges are shown.

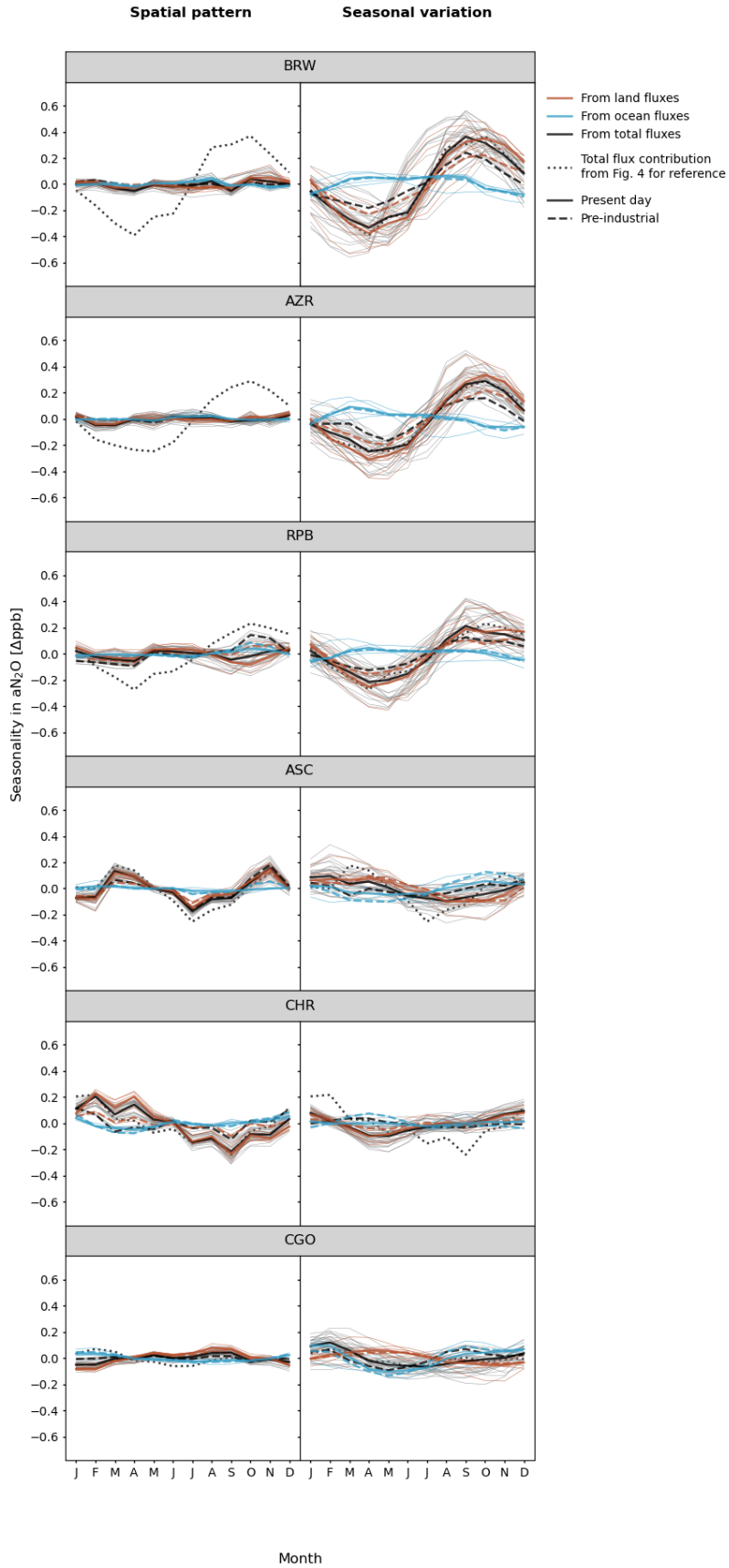


Figure S3. Same as Figure 4 but for additional stations. Modeled aN₂O seasonality at different NOAA/CCGG flask stations (BRW: Barrow, AZR: Terceira Island, RPB: Ragged Point, CHR: Christmas Island, ASC: Ascension Island, CGO: Cape Grim) from spatial pattern (12-month running mean) and seasonal variation (detrended fluxes) of N₂O fluxes for pre-industrial period (1861-1880; dashed lines) and present day (2001-2020; solid lines). The aN₂O seasonality modeled from total (including both spatial and seasonal variations) land and ocean N₂O emissions of present day are repeated for reference in all panels.

Reference

EDGAR (Emissions Database for Global Atmospheric Research) Community GHG Database (a collaboration between the European Commission, Joint Research Centre (JRC), the International Energy Agency (IEA), and comprising IEA-EDGAR CO₂, EDGAR CH₄, EDGAR N₂O, EDGAR F-GASES version 8.0, (2023) European Commission.